논문 2007-44TC-12-2

1차원 RLH-TL 방사효과 모델링 및 해석

(Modeling and analysis of radiation effects for 1-D RLH-TL)

문 효 상*, 이 범 선**

(Hyosang Moon and Bomson Lee)

요 약

본 논문에서는 기존의 Right/left-handed 전송선(RLH-TL)에 집중 직렬 캐패시터와 병렬 인덕터 구현으로 발생하는 방사효과를 포함하여 단위 셀을 모델링한다. 방사 효과가 고려된 RLH-TL 단위셀의 등가 회로를 제공하고 갭 커패시터와 션트 인더터에서의 방사율에 따른 Bloch 임피던스와 복소 전파상수를 해석한다. 두 개의 방사율이 같을 때 RLH-TL의 Bloch 임피던스는 RH-TL의 특성임피던스와 같아짐을 보인다. 게다가, 주어진 주파수에서 특정한 위상 변화를 위한 단위 셀의 설계 공식을 유도하여 제공한다. 마지막으로, 안테나 응용을 위해 RLH-TL에서 다양한 방법으로 방사효과를 control할 수 있는 설계 공식을 제공한다.

Abstract

This paper presents the radiation rate formula due to inclusion of a series capacitor and shunt inductor in a unit cell for the right/left-handed transmission line (RLH-TL). The equivalent circuit for a RLH unit cell considering radiation effects is presented and analyzed in terms of the Bloch impedance and dispersion diagram. It has been found that when two radiation rates are identical, the Blockimpedance reduces to the characteristic impedance of the host conventional RH-TL. Besides, design equations for a unit cell for a specific phase shift at a given frequency are provided. The method of realizing uniform excitation along the RLH-TL is also proposed for antenna applications.

Keywords : Metamaterial Transmission Line

Ⅰ. Introduction

There has been intense research on metamaterial-based transmission lines. The conventional transmission lines, which usually support TEM waves and follow the right hand rule (right-handedness), have been characterized by the distributed series inductance L (given in unit of H/m) and shunt capacitance C (given in unit of F/m). By adding a lumped-type series capacitance C_0 and shunt inductance L_0 periodically with a unit cell size of d much smaller than the wavelength, the composite right- and left hand-handed transmission line can be constructed and many applications in the microwave band have followed[1~6]. The lumped series capacitance C_0 has been commonly realized by a transverse cut or interdigital cut on the signal line, while the lumped shunt inductance L_0 has been commonly realized by a shunt shorted stub. In realizing C_0 periodically on the line, some power is leaked out of the cuts. In realizing L_0, some power is also leaked out of the shorted stub due to a discontinuity problem. These radiation losses are inevitable. For most applications such as phase

* 학생회원, ** 정회원, 경희대학교 전자정보대학
(School of Electronics and Information, Department of Radio Communication Engineering, Kyunghee University)
※ This work was supported by the Korea Science and Engineering Foundation (KOSEF) grant NO. R01-2007-000-11567-0.
접수일자: 2007년11월28일, 수정완료일: 2007년12월12일

shifters, directional couplers, power dividers, and etc, this radiation effect be haves adversely to their desired performances since the transmitted power levels are usually somewhat less than the required ones. For these applications, design must be carried out to minimize the radiation losses. The minimization of the radiation losses is possible although it is limited. For antenna applications such as leaky wave antennas, these radiation effects need to be controlled. Some beneficial features of leaky wave antennas have been widely reported, while some refining study still needs to be performed further. In this paper, radiation effects are studied and considered in the proposed equivalent unit cell. The radiation rate formula for the series gap capacitor and shunt stub inductor is derived using transmission line theory. The equivalent circuit is examined in terms of the Blockimpedance of complex propagation constant. Some design equations for control of radiated power are also presented.

Ⅱ. Modeling and analysis of equivalent circuit for RLH-TL considering radiation effects

We will start the analysis from the parallel-plate transmission line loaded with a series capacitor with C_0 and shunt inductor with L_0 as shown in Fig. 1 since the mapping relations between the circuit and field parameters are simply determined by the cross-section geometry (width W and height h).

Without the loading of C_0 and L_0, the RLH-TL as shown in Fig. 1 simply becomes the conventional

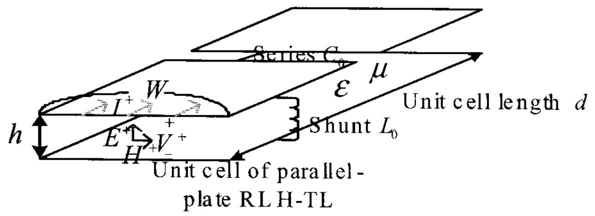

그림 1. 직렬 캐패시터와 병렬 인덕터를 가지는 평행판 전송 선로의 단위 격자 모델

Fig. 1. Unit cell model for parallel-plate transmission line with series capacitor and parallel inductor.

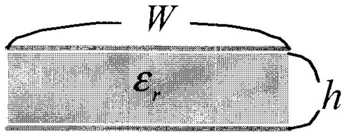

$$g=\frac{h}{W}$$

(a) 평행도체판 전송선

(a) parallel-plate transmission line

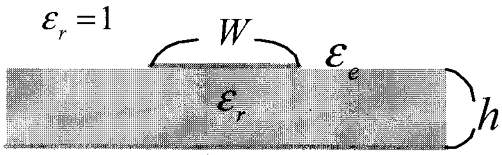

$$g=\frac{1}{2\pi}\ln\left(\frac{8h}{W}+\frac{W}{4h}\right) for \frac{W}{h}\le 1$$

$$=\frac{1}{\frac{W}{h}+1.393+0.667\ln\left(\frac{W}{h}+1.444\right)} for \frac{W}{h}\ge 1$$

(b) 마이크로스트립라인

(b) microstrip line

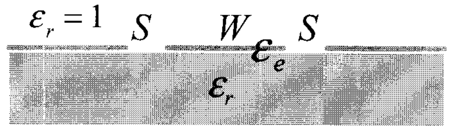

$$g=\frac{K'}{4K}$$

where $\frac{K}{K'}=\frac{1}{\pi}\ln\left(2\frac{1+\sqrt{k}}{1-\sqrt{k}}\right),\ 0.7\le k<1$

$$\frac{K}{K'}=\left[\frac{1}{\pi}\ln\left(2\frac{1+\sqrt{k'}}{1-\sqrt{k'}}\right)\right]^{-1},\ 0<k\le 0.7$$

$$k=\frac{W}{W+2S},\quad k'=\sqrt{1-k^2}$$

(c) CPW 라인

(c) CPW line

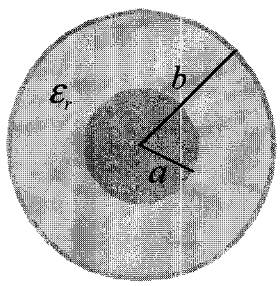

$$g=\frac{\ln(b/a)}{2\pi}$$

(d) 동축 전송선

(d) coaxial transmission line

그림 2. 다양한 전송 선로의 기하학적인 요소

Fig. 2. Geometrical factor for various transmission lines.

right-handed transmission line (RH-TL). For the unloaded lossless transmission line, the distributed series inductance $L(H/m)$ and shunt inductance C (F/m) are given by

$$L = \mu\frac{h}{W} = \mu g(H/m) \qquad (1)$$

and

$$C = \varepsilon\frac{W}{h} = \frac{\varepsilon}{g}(F/m) \qquad (2)$$

where g is the geometrical factor. For TEM RH-TL, the characteristic impedance Z_c is given by the product of the intrinsic impedance η and the geometrical factor g :

$$Z_c = \frac{V^+}{I^+} = \frac{E^+h}{H^+W} = \sqrt{\frac{\mu}{\varepsilon}}\frac{h}{W} = \eta g = \sqrt{\frac{L}{C}}(\Omega) \qquad (3)$$

The geometrical factors for various kinds of transmission lines are summarized in Fig. 2.

The intrinsic impedance η is given by $\sqrt{\mu_0/(\varepsilon_0\varepsilon_e)}$ and ε_e(see Fig. 2) is the effective relative permittivity. For the parallel-plate and coaxial lines, $\varepsilon_e = \varepsilon_r$. For the microstrip and CPW lines, refer to [7]

For an ideal lossless RLH-TL with loading of C_0 and L_0, the important analysis equations are given by

$$LC = \mu\varepsilon = \mu_0\varepsilon_0\varepsilon_e \qquad (4)$$

$$Z_c = \sqrt{\frac{L}{C}} = \sqrt{\frac{L_0}{C_0}} \text{ (matching condition)} \qquad (5)$$

and

$$(-\beta d) \approx -\left(\omega\sqrt{LC}d - \frac{1}{\omega\sqrt{L_0C_0}}\right) = \phi_\omega(rad) \qquad (6)$$

(phase shift per unit cell at a radian frequency of ω)

For a specific phase shift ϕ_ω per unit cell at a radian frequency of ω, the design equations for the C_0 and L_0 loadings can be obtained as

$$C_0 = \frac{1}{Z_c}\frac{1}{\omega^2\sqrt{LC}d + \omega\phi_w} = \frac{1}{Z_c}\frac{1}{\omega^2\sqrt{\varepsilon_e}d/c + \omega\phi_w} \qquad (7)$$

and

$$L_0 = Z_c^{\,2}C_0 \qquad (8)$$

where c is the speed of light and ε_e is the relative effective permittivity.

Most design employing metamaterial-based transmission lines is now based onthe lossless equivalent circuit, although some optimization trial follows to deal with losses through EM simulation and actual measurement.

The lumped series capacitance C_0 can be realized by a transverse cut or interdigital cut on the signal line, while the lumped shunt inductance L_0 can be realized by a shunt shorted stub. In realizing C_0, some power is leaked out of the cuts. In a trial to consider this radiation effect, a lumped resistor R_0 has been included as shown in Fig. 3(a), where the total lumped impedance Z_0 is given by

$$Z_0 = R_0 + \frac{1}{j\omega C_0} = \frac{1}{j\omega C_0}[1 + jp_1(\omega)](\Omega) \qquad (9)$$

In (9), the perturbation factor p_1 for radiation due to the series loading of C_0 is defined as

$$p_1(\omega) = \frac{R_0}{1/(\omega C_0)} \qquad (10)$$

as a ratio of the resistance R_0 and impedance magnitude of C_0.

The radiation rate η_1 due to the series loading of C_0 can be calculated to be

$$\eta_1 = \frac{P_{rad1}}{P_{in}} = \frac{\frac{|V|^2}{2}\mathrm{Re}(Y_0)}{\frac{|V_1^+|^2}{2Z_c}} = \frac{4\omega C_0Z_cp_1(\omega)}{|2\omega C_0Z_c - j[1 + jp_1(\omega)]|^2} \approx \frac{R_0}{Z_c} \qquad (11)$$

if $\frac{1}{\omega C_0} \ll Z_c$, which is indeed true for most practical cases. Since the radiation rate η_1 due to inclusion of C_0 has turned out to be independent of frequency, we prefer to use the radiation rate η_1 also as a perturbation factor instead of p_1.

The distributed series impedance per unit length may now be written by

$$\begin{aligned} Z &= j\omega L + \frac{1}{j\omega C_0}/d + R_0/d \\ &= j\omega\left(L - \frac{1}{\omega^2 C_0 d}\right) + (\eta_1 Z_c)/d \\ &= j\omega L_{eff} + (\eta_1 Z_c)/d\ (\Omega/m) \end{aligned} \quad (12)$$

The effective distributed series inductance L_{eff} may be positive, zero, and negative depending on the degree of added left-handedness due to periodic L_0 loading in a unit cell size d.

In realizing L_0, some power is also leaked out of the shorted stub due to a discontinuity problem. To deal with this effect, a lumped conductance G_0 has been included as shown in Fig. 3(b).

The derivation for the radiation rate η_2 due to inclusion of a shunt stub inductor L_0 similarly goes with the one for η_1 due to inclusion of a series capacitor C_0. The radiation rate due to a stub inductor can be shown to be given by

$$\eta_2 \approx \frac{G_0}{Y_c} \quad (13)$$

The distributed shunt admittance per unit length may now be written as

$$\begin{aligned} Y &= j\omega C + \frac{1}{j\omega L_0}/d + G_0/d \\ &= j\omega\left(C - \frac{1}{\omega^2 L_0 d}\right) + (\eta_2 Y_c)/d \\ &= j\omega C_{eff} + (\eta_2 Y_c)/d\,(\mho/m)\ . \end{aligned} \quad (14)$$

The effective distributed shunt capacitance C_{eff} may be positive, zero, and negative depending on the degree of added left-handedness due to periodic L_0 loading in a unit cell size d. The effective distributed series inductance L_{eff} and shunt capacitance C_{eff} (circuit parameters) are related with the effective relative permeability μ_{eff} and permittivity ε_{eff} as follows.

$$L_{eff} = \mu_0 \mu_{eff} \frac{h}{W} = \mu_0 \mu_{eff}\, g(H/m) \quad (15)$$

$$C_{eff} = \varepsilon_0 \varepsilon_{eff} \frac{W}{h} = \varepsilon_0 \varepsilon_{eff} / g(F/m) \quad (16)$$

L_{eff} is seen to be proportional to μ_{eff} with the proportionality constant μ_0g and C_{eff} is seen to be proportional to ε_{eff} with the proportionality constant ε_0/g. The pair of L_{eff}(or μ_{eff}), C_{eff}(or ε_{eff}) may be both positive (Double Positive(DPS) : RH region), both negative (Double Negative(DNG): LH region), only μ_{eff} (or L_{eff}) negative (Mu Negative(MNG)), or only ε_{eff} (or C_{eff}) negative (Epsilon Negative(ENG)) depending on the degree of added left-handedness (LH) to the host RH-TL.

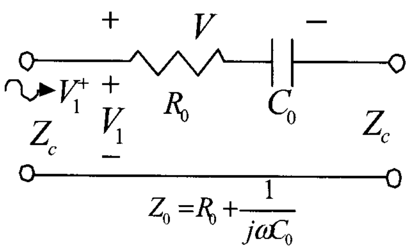

(a) 직렬 커패시터
(a) series gap capacitor

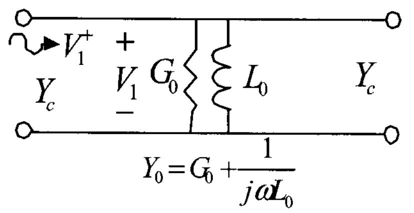

(b) 션트 인덕터
(b) shunt inductor

그림 3. 직렬 캐패시터와 병렬 인덕터의 등가 회로
Fig. 3. Equivalent circuit for series capacitor and shunt inductor.

The total radiation rate η due to a gap capacitor and stub inductor is the sum of each and given by

$$\eta = \eta_1 + \eta_2 = \frac{R_0}{Z_c} + \frac{G_0}{Y_c} \qquad (17)$$

This result can be also verified from the expression of α for lossy TL given by

$$\alpha = \frac{1}{2}\left(\frac{R}{Z_c} + \frac{G}{Y_c}\right) \qquad (18)$$

where R and G are the distributed series resistance and shunt conductance per unit length, respectively.

Along the lossy (or leaky) TL, the power flow at a specific position can be written as

$$P(z) = P_0 e^{-2\alpha z} \qquad (19)$$

Total radiation rate in a unit cell leads to the same result

$$\eta = \frac{P_0(1-e^{-2\alpha d})}{P_0} = 1 - e^{-2\alpha d} = 1 - e^{-\left(\frac{R_0}{Z_c} + \frac{G_0}{Y_c}\right)}$$

$$\xrightarrow{\frac{R_0}{Z_c} + \frac{G_0}{Y_c} \ll 1} \frac{R_0}{Z_c} + \frac{G_0}{Y_c} = \eta_1 + \eta_2 \qquad (20)$$

In Fig. 4, we show the equivalent circuit of a unit cell considering radiation effects. The right-handed transmission line (RH-TL) with its electrical length kd is usually characterized by the distributed series inductance L(H/m), series resistance R(Ω/m), shunt capacitance C(F/m), and shunt conductance G(℧/m). The left-handedness comes from C_0 and L_0 but they are inevitably accompanied by R_0 and G_0. For most

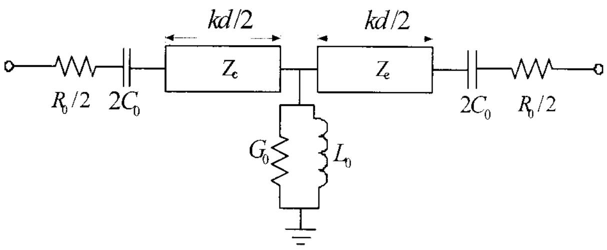

그림 4. 방사효과를 고려한 단위 셀의 등가회로

Fig. 4. Equivalent circuit of a unit cell considering radiation effects.

practical applications, $R \ll \frac{R_0}{d}$ and $G \ll \frac{G_0}{d}$, and thus we will assume that $R = G = 0$ throughout our analysis.

The Bloch impedance Z_B, which differs from the characteristic impedance due to loading effects of C_0 and L_0, is related with the ratio of Z (12) and Y (14) as given by

$$Z_B = \sqrt{\frac{Z}{Y}} = \sqrt{\frac{j\omega\left(L - \frac{1}{\omega^2 C_0 d}\right) + (\eta_1 Z_c)/d}{j\omega\left(C - \frac{1}{\omega^2 L_0 d}\right) + (\eta_2 Y_c)/d}} \qquad (21)$$

and plotted in Fig. 5(a) (real part) and 5(b) (imaginary part) as a function of frequency for the case of C_0=3.355pF, L_0=3.3875nH, $Z_c = \sqrt{L/C} = \sqrt{L_0/C_0} = 50\Omega$, $LC = 1/c^2$ and $kd = 2\pi/20$ at 3GHz . For the case of no radiation ($\eta_1 = \eta_2 = 0$), the Bloch impedance Z_B is shown to reduce to the characteristic impedance Z_c(Re(Z_B) = 50Ω and Im(Z_B) = 0Ω) in the wide frequency region about the transition frequency of 3GHz. When η_1= 0.02 and η_2 = 0, $Z \rightarrow (0.02 Z_c)/d$ and $Y \rightarrow 0$ near the transition frequency of 3GHz. Besides, since the numerator is positively finite and denominator goes to zero, Re(Z_B) $\gg Z_c$ and |Im(Z_B)| $\gg 0$ changing sign near the transition frequency of 3GHz. The behaviors of Z_B for other radiation rates may be understood by observing the property coming from the division Z/Y. One thing particular about Z_B is that when the radiation rates η_1 and η_2 are the same (let us say $\eta_1 = \eta_2 = 0.02$), $Z_B \rightarrow Z_c$. This means that if the degrees of radiation due to the transverse cut (for C_0) and the shorted stub (for L_0) characterized by η_1 and η_2 are the same, there is a perfect match at the input connecting the RH transmission line and RLH loaded transmission line. Usually, the typical radiation rates are approximately in the range 0.01-0.1 (1-10%) depending on loading structures. The control of the radiation rate η_1 is usually easier

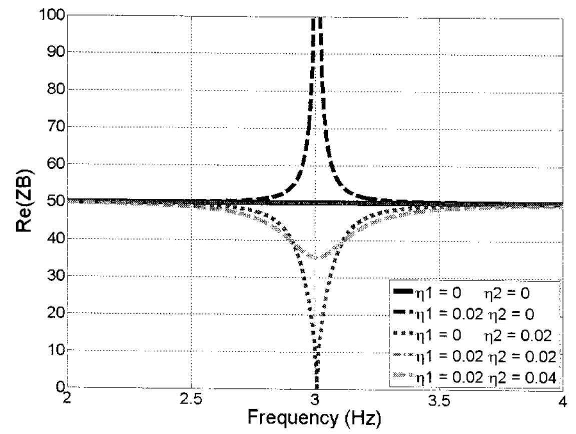

(a) Z_B의 실수부

(a) Re(Z_B)

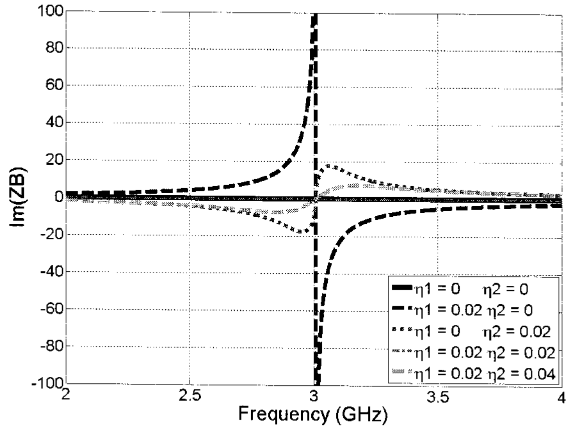

(b) Z_B의 허수부

(b) Im(Z_B)

그림 5. 다른 방사율 η_1과 η_2를 갖는 경우 주파수에 따른 Bloch 임피던스

Fig. 5. Bloch impedance as a function of frequency for different radiation rates η_1 and η_2

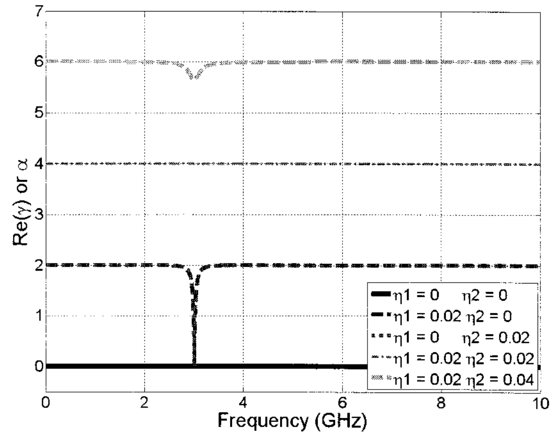

(a) 감쇄 상수 α

(a) attenuation constant α

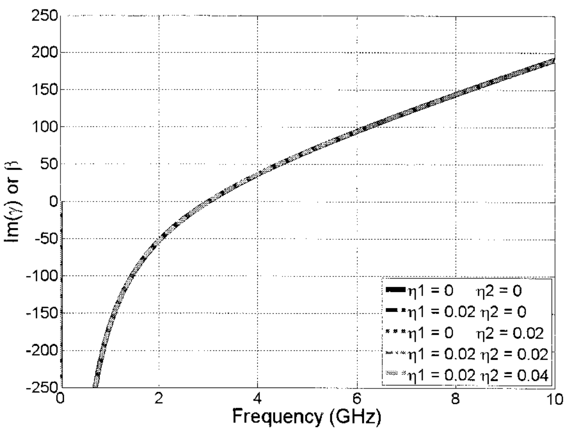

(b) 전파 상수 β

(b) propagation constant β

그림 6. 다른 방사율 η_1과 η_2를 갖는 경우 주파수에 따른 복소 전파상수

Fig. 6. Complex propagation constants as a function of frequency for different radiation rates η_1 and η_2.

than the control of η_2. Thus, the realization of L_0 is recommended in advance of C_0. If L_0 is realized on any TEM transmission line with a specific radiation rate η_2, then we need to make an effort to obtain the same radiation η_1 as η_2 by adjusting the transverse cut for C_0.

The complex propagation constant γ is related with the product of Z and Y and given by

$$\gamma = \sqrt{ZY} \tag{22}$$

The real (α) and imaginary part (β) of γ are plotted in Fig. 6(a) and 6(b) as a function of frequency. The attenuation constant α in Fig. 5(a) is almost flat and can be shown to agree with

$$\alpha = \frac{1}{2d}\left(\frac{R_0}{Z_c} + \frac{G_0}{Y_c}\right) = \frac{1}{2d}(\eta_1 + \eta_2) = \frac{\eta}{2d} \tag{23}$$

except at the transition frequency of 3GHz. When η_1 = 0.02 and η_2 = 0 or vice versa, the attenuation constant α is shown to become very small near the transition frequency of 3 GHz. However, this will not happen in practical situations since any transverse cuts or discontinuities on the transmission line more or less cause some radiation. The propagation

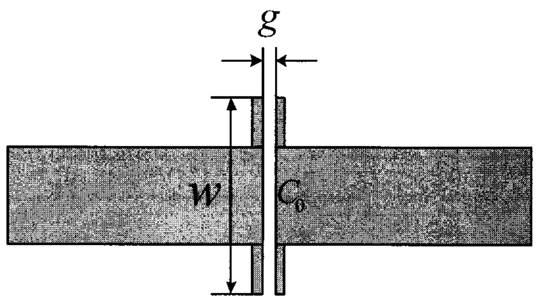

그림 7. 갭 커패시터의 구조
Fig. 7. Geometry of gap capacitor.

constant β is shown to be almost the same for all cases of small radiation considered.

The control of radiation rate η_1 is possible by adjusting the width w and gap g shown in Fig. 7

The gap capacitance C_0 in Fig. 7 is proportional to the ratio of w/g and radiation from the gap increases as w increases. Thus, the control of radiation rate η_1 is possible by a proper choice of w and g.

Ⅲ. Power control for antenna applications

For antenna applications (leaky wave antenna for an example), we need to design a RLH unit cell such that $\eta_1 = \eta_2$ as much as possible. If this is the case, $Z_B \rightarrow Z_c$ and the periodically loaded RLH-TL is completely matched to the unloaded input RH-TL. In a periodic RLH-TL with identical unit cells, power leaking out of the each unit cell decreases exponentially. The total radiated power up to the Nth cell ($\eta_{T,N}$) is given by

$$\eta_{T,N} = 1 - e^{-\eta N} \tag{24}$$

where η is the total radiation rate for a unit cell.

If a specific $\eta_{T,N}$ is desired, the total required number N of the unit cells is obtained by

$$N = \frac{\ln(1-\eta_{T,N})}{\eta} \tag{25}$$

The uniformly radiating array may be more frequently needed than the exponentially radiating array. This is possible with non-uniform radiation rates along the transmission line given by

$$\eta_n = \frac{\eta_0}{1-n\eta_0} (n = 0,1,2,\cdots) \tag{26}$$

where η_0 is the radiation rate referred to the input power reaching the first unit cell and the total required number N of the unit cells for a specific $\eta_{T,N}$ is given by

$$N = \frac{\eta_{T,N}}{\eta_0} \tag{27}$$

Ⅳ. Conclusions

We have modeled and analyzed the equivalent circuits for the RLH-TL considering radiation effects in terms of the Bloch impedance and dispersion diagram. The radiation rate formula has been derived, which explains the inclusion effects of a series capacitor and shunt inductor in a unit cell for the right/left-handed transmission line (RLH-TL). It has been found that when two radiation rates are identical, the Bloch impedance reduces to the characteristic impedance of the host RH-TL. Besides, design equations for a unit cell for a specific phase shift at a given frequency have been provided. The method of realizing uniform excitation along the RLH-TL has also been proposed for antenna applications.

References

[1] Marco A. Antoniades, George V. Eleftheriades, “Compact linear lead/lag metamaterial phase shifters for broadband applications”, Antennas and Wireless Propagation Letters, vol. 2, no. 1, pp 103-106, 2003.
[2] Sungjoon Lim, Christophe Caloz, Tatsuo Itoh, “Metamaterial-based electronically controlled transmission-line structure as a novel leady-wave antenna with tunable radiation angle and beamwidth”, IEEE Trans. Microwave Theory Tech, vol. 53, no. 1, pp161-173, Jan. 2005.
[3] Christophe Caloz, and Tatsuo Itoh, “A novel

mixed conventional microstrip and composite right/left-handed backward-wave directional coupler with broadband and tight coupling characteristics", IEEE Microw. Wireless Compon. Lett., vol. 14, no. 1, Jan. 2004.

[4] Rubaiyat Islam, George V. Eleftheriades, "Phase-agile branch-line couplers using metamaterial lines", IEEE Microw. Wireless Compon. Lett., vol. 14, no. 7, July 2004.

[5] Rubaiyat Islam and George V. Eleftheriades, "A planar metamaterial co-directional coupler that couples power backwards", IEEE MTT-S Digest, vol. 3, 2003.

[6] George V. Eleftheriades, Ashwin K. Iyer, and Peter C. Kremer, "Planar negative refractive index media using periodically L-C loaded transmission lines;", IEEE Trans. Microwave Theory Tech, vol. 50, Issue 12, Dec. 2002.

[7] Robert E. Collin, Foundations for Microwave Engineering, 2 ed., Eagle-wood Cliffs, NJ, McGraw-Hill, 1992.

저 자 소 개

문 효 상(학생회원)
2006년 2월 숭실대학교 정보통신 전자공학부 (공학사)
2006년 3월～현재 숭실대학교 정보통신공학과 석사과정
<주관심분야 : Metamaterial TL 이론, 소형 광대역 안테나 설계, RFID Tag 등>

이 범 선(정회원)
1982년 2월 서울대학교 전기공학과 (공학사)
1991년 8월 미국 네브래스카주립대 전자공학과 (공학석사)
1995년 5월 미국 네브래스카주립대 전자공학과 (공학박사)
1995년 5월～1995년8월 미국 네브래스카주립대 포닥(Post Doctor)
1995년 9월～현재 경희대학교 전자정보대학 교수
<주관심분야 : 초고주파 수동소자(Metamaterial), 소형안테나(RFID 태그 안테나 등) 등>